Real-Time Prototyping of Optimal Experiment Design in Power Systems using Modelica and FMI

Marcelo de Castro
Rensselaer Polytechnic Institute
Troy, NY, USA
Email: decasm3@rpi.edu

Sjoerd Boersma
Wageningen University & Research
Wageningen, Netherlands
Email: sjoerd.boersma@wur.nl

Luigi Vanfretti
Rensselaer Polytechnic Institute
Troy, NY, USA
Email: vanfrl@rpi.edu

***Abstract*—System identification techniques are incredibly valuable for power system applications. Recent techniques have explored the optimal design for excitation signals in order to maximize an objective function related to an identification procedure. In this context, this paper presents a framework for the deployment of optimal experiment design in power systems using real-time simulation-based experiments. As a first step towards hardware-in-the-loop prototyping of probing experiments, power system models designed with Modelica are exported via FMI standard for deployment in real-time simulators. Results from the real-time simulator show optimized probing signals and provides insights on the chosen optimization weights. The portability of the studied model allows the identification technique to be tested in the real-time simulator environment for probing signal design optimization before field experiments are conducted.**

I. Introduction

Modern power systems need to comply with very unyielding performance standards due to reliability concerns and, therefore, careful analysis on these networks is carried out. Traditionally, these analyses are conducted relying on mathematical models of power networks from proprietary software tools that, in the past, have been shown to capture the main dynamics that should be observed in measurements made in the field [1]. However, this task is becoming more arduous as the power system scale and complexity increases, specially when new power electronic devices are connected to the grid as part of the on-going energy transition.

In order to assist engineers in this difficult task, advanced mathematical techniques have been applied for system identification in power networks. This allows engineers to improve their models while relying on field measurement data being observed in the real power grid. In the past, simulation-based studies to use those techniques were implemented by simulating ambient noise [2] due to load changes, for example [1]. The main reason behind that is because experiments to inject test signals could need careful planning to avoid any potential danger that would compromise the safe operation of the network, consequently, their cost is non-negligible.

To date, many different experiments have been safely conducted with the injection of probing signals for the purpose of identification. Results have shown that depending on the design of the excitation signal, the quality of the estimation will vary. Experiments have been conducted with standardized excitation signals which are manually chosen to be applied in real-world networks for damping estimation [3] or general network characterization [4]. However, when applying an excitation signal with frequency content close to a critical mode frequency, the oscillations might become dangerously large [5]. Hence, there is an obvious necessity to carefully select the frequency content of the excitation signal in order to guarantee a good estimation quality, while maintaining the grid in a safe operating condition.

This motivates the study of optimized signals that are designed to excite the system while minimizing the impact on the power system. Previous research has addressed this by pre-filtering excitation signals before injecting them, aiming to minimally impact the network [6], [7]. Moreover, multi-sine signals can be optimized to obtain excitation signals with small amplitudes while having pre-determined power spectrum [8] or to produce minimal network disturbance while ensuring an appropriate damping estimate [9], [10].

The aforementioned previous studies have been carried out using off-line simulators, where the probing signal and actuator are also simulated. Naturally, this approach will not be able to address issues related to real-world signal realization in hardware and the actuator's response in real-time as it is applied in the field. To address such issues, the real-time (RT) hardware-in-the-loop (HIL) approach can be exploited [11]. This paper takes a first step to address this gap, it presents an optimal probing design using Modelica [12] and the Functional Mock-Up Interface (FMI) standard [13] to create a RT simulation prototype to test the probing design solution in hardware. The real-time experiment allows many experiments to be performed with a high fidelity for the assessed measurements that are obtained from the RT simulation. We exploit the portability of the Functional Mock-up Units (FMUs) to reduce the need of model re-implementation between off-line and RT design tasks, which allows to use different software platforms with minimum effort. In this study, the RT experiment is conducted using a dSPACE SCALEXIO LabBox.

This paper is organized as follows: Section II summarizes all the fundamentals about system identification used in this work; Section III describes the models in Modelica, their export

This work was funded in part by the New York State Energy Research and Development Authority (NYSERDA) under grant agreement numbers 37951, in part by Dominion Energy, and in part by the Center of Excellence for NEOM Research at King Abdullah University of Science and Technology.

using FMI and how they are implemented in the RT simulation experiment set-up; Section IV presents the results obtained in the experiment while Section V draws the final remarks of this work.

II. Power System Identification

A. Network Dynamics Description

The nonlinear dynamic process that defines a general electrical power network can be written as

$$\begin{cases} \dot{x}(t) &= f(x(t), u(t), w(t), t), \\ y(t) &= g(x(t), u(t), v(t), t), \end{cases} \tag{1}$$

where $f(\cdot)$ and $g(\cdot)$ are unknown time-varying nonlinear functions, t is time, $x(t) \in \mathbb{R}^{n_x}$ is the state variable of the network, $u(t) \in \mathbb{R}^{n_u}$ are the control or excitation signal, $y(t) \in \mathbb{R}^{n_y}$ is the measurement variable and $w(t) \in \mathbb{R}^{n_w}$ and $v(t) \in \mathbb{R}^{n_v}$ are the non-measurable process and the measurement noise, respectively. Notice that the latter comes from the actual measurement devices and it only affects $y(t)$, while $w(t)$ acts on the states and therefore, it changes the dynamic behavior of the network.

B. System Identification

System identification aims at finding a continuous- or discrete-time reduced order model that describes the dominant characteristics from Eq. (1). This identified model can be described by

$$\begin{cases} \dot{\hat{x}}(t) &= \hat{f}(\hat{x}(t), u(t), \hat{w}(t), \hat{\theta}_N(t)), \\ \hat{y}(t) &= \hat{g}(\hat{x}(t), u(t), \hat{v}(t), \hat{\theta}_N(t)), \end{cases} \tag{2}$$

where $y(t)$ and, potentially, $u(t)$ come from Eq. (1), the reduced state vector is $\hat{x}(t) \in \mathbb{R}^{n_{\hat{x}}}$ ($n_{\hat{x}} << n_x$), the identified parameter vector is $\hat{\theta}_N \in \mathbb{R}^{n_\theta}$, the estimations of process is $\hat{w}(t)$ and measurement noise is $\hat{v}(t)$, and N is the amount of data points are used in the identification procedure. Noise terms are also used to model uncertainty, discretization errors and non-modeled dynamics.

Generally, linear system identification techniques are attractive due to their simplicity and, in this work, a black-box-based system identification technique called Predictive Error Method (PEM) is employed [14], [15]. It estimates Eq.(2) as

$$\hat{y}(k) = \hat{G}(z, \hat{\theta}_N)u(k) + \underbrace{\hat{H}(z, \hat{\theta}_N)e(k)}_{\bar{v}(k)}, \tag{3}$$

with $z \in \mathbb{C}$, $\hat{G}(z, \hat{\theta}_N), \hat{H}(z, \hat{\theta}_N)$ discrete-time transfer functions and k the discrete time. Note that in (3), the process and measurement noise are modeled together in $\bar{v}(k)$ with unknown $e(k)$ zero-mean white noise. In addition, with PEM the number of poles and zeros in (3) are pre-defined by the analyst. The variance of the frequency response of $\hat{G}(z, \hat{\theta}_N)$ [16] can be approximated by

$$\text{variance}\left(\hat{G}(\omega, \hat{\theta}_N)\right) \approx n_{\hat{x}} \frac{\Phi_v(\omega)}{N\Phi_u(\omega)}, \tag{4}$$

with $n_{\hat{x}}$ the user-defined model order of $G(z, \hat{\theta}_N)$, frequency ω and $\Phi_v(\omega), \Phi_u(\omega)$ the power spectrum of the noise $\bar{v}(k)$ and excitation signal $u(k)$, respectively. Note from in (4) that increasing N or the power level of the excitation signal will lead to a decreasing variance.

The identification procedure employed in this work uses an objective function in order to measure how well the model fits the experimental data. The identification criterion used is shown in Eq.(5).

$$V(\hat{y}(k), y(k), u(k), \theta) = \frac{1}{N}\sum_{k=1}^{N} \varepsilon^2(k, \theta). \tag{5}$$

The parameters of $\hat{G}(\omega, \hat{\theta}_N)$ are estimated by solving

$$\hat{\theta}_N = \arg \min_{\theta} V\big(\hat{y}(k), y(k), u(k), \theta\big), \tag{6}$$

where the residual $\varepsilon(k, \theta)$ is defined as

$$\varepsilon(k, \theta) = H(z, \hat{\theta}_N)^{-1}\left(y(k) - G(z, \hat{\theta}_N)u(k)\right). \tag{7}$$

C. Optimal Experiment Design

The goal in this paper is to accurately estimate a measurement-based reduced order model of the power system capable of representing its electro-mechanical dynamics by applying a probing signal to an available input $u(t)$, similar to [8], with the additional requirements of limiting the variance of $\hat{\theta}_N$ while minimizing the power of $u(t)$ and $y(t)$.

To achieve this goal, the model structure adopted to study the power network is presented in [10] and it assumes that a mode can be represented by the sample period h and by the pair $(\zeta_i, \omega_{n,i})$, where the former is the damping and the latter is corresponding frequency of mode $i \in [1, n_i]$, with n_i being the number of modes.The optimized signal $u(t)$ should ensure an upper bound on the variance of $\hat{\theta}_N$, i.e. $(\hat{\zeta}_i, \hat{\omega}_{n,i})$, while minimizing the power in the excitation signal $u(t)$ and measurement $y(t)$ [10]. The optimized $u(t)$ is, assuming an ARMAX model structure, found by solving

$$\begin{aligned} \min_{A_r^2(r=1,\ldots,M)} \quad & \overbrace{\frac{c_1}{2}\sum_{r=1}^{M} A_r^2}^{c_1\cdot\text{power in } u(t)} + \overbrace{\frac{c_2}{2}\sum_{r=1}^{M} A_r^2 \left|\hat{G}(\omega_r, \hat{\theta}_N)\right|^2}^{c_2\cdot\text{power in } y(t)}, \\ \text{subject to :} \quad & \text{variance}(\zeta_i) < \eta_i, \quad \text{for} \quad i = 1, \ldots, n_i, \\ & A_r^2 \geq 0, \qquad\quad \text{for} \quad r = 1, \ldots, M, \end{aligned} \tag{8}$$

with user-defined frequency grid ω_r for $r = 1, \ldots, M$ and η_i is the analyst-defined upper-bound to this damping value ζ_i. Weights c_1 and c_2 allow the analyst to target either the minimization of the power in $u(t)$ or $y(t)$. The multi-sine optimized excitation signal $u(t)$ is, then, defined as

$$u(t) = \sum_{r=1}^{M} A_r \cos(\omega_r t + \varphi_r), \tag{9}$$

where φ_r is the phase of the sinusoidal component defined by the analyst. Its power spectrum is defined as

$$\Phi_u(\omega) = \frac{\pi}{2}\sum_{r=1}^{M} A_r^2 \left[\delta(\omega - \omega_r) + \delta(\omega + \omega_r)\right], \tag{10}$$

with $\delta(\cdot)$ the Dirac function. Note that while frequency ω_r and phase φ_r are analyst-defined, the amplitude A_r is found via the optimization of Eq. (8) for all frequency points in the grid ω_r. Moreover, observe that by using the multi-sine signal in Eq. (9) it is relatively simple to reduce the identified model's variance for a determined frequency of interest. It is also easy to reduce the power of $u(t)$ at high frequencies, which allows to minimize potential interference with other dynamics whose frequency are outside the target range for identification.

D. Model Validation

After the optimal experiment is conducted, it is necessary to validate the identified model by investigating its statistical properties. As shown in Eq. (4), PEM provides mathematical expressions for an estimation of the model's variance. This property can be used to assess if the identified model satisfies the specified criteria. Moreover, time-domain data is compared in order to produce a fit value between collected validation data $y_{\text{val}}(t)$ and the identified model's output $\hat{y}(t)$, as

$$\text{fit} = \left[1 - \frac{(y_{\text{val}}(t) - \hat{y}(t))^2}{(y_{\text{val}}(t) - \mu_{y_{\text{val}}})^2}\right] \cdot 100\%, \tag{11}$$

where μ_y the mean of the validation data $y_{\text{val}}(t)$. To avoid overfitting, validation and identification data should be distinct.

III. Real-Time Experiment Setup

In this study, two experiments are conducted. Each experiment has different weights c_1 and c_2 and two batches of data, because Eq. (8) requires an identified ARMAX model for optimization. The first batch applies an excitation signal $u(t)$ selected by the analyst and that has not been optimized. The amplitudes A_r during this first batch are manually chosen such that a validated initial model is obtained, which can be used in (8). Note that the values of A_r cannot be smaller than a threshold, otherwise the resulting model would not be a validated one and, therefore, cannot be used in (8). The resulting identified model is then used to find the optimized excitation signal, which is then injected in the network when the second batch is being acquired, and is used in the identification procedure. In this context, the RT simulator is useful for creating a first ARMAX model without actually injecting signal into a real network.

Although real power networks are typically very large, this experiment considers a much simpler example system in order to demonstrate the RT experiment set-up. The Single Machine Infinite Bus (SMIB) test network consists of very few elements: three buses, two lines, one transformer and one machine. Its diagram is shown in Fig. 1a, while its Modelica implementation using the OpenIPSL [17] is shown in Fig. 1b.

To inject signals during the RT simulation, using the model in Fig. 1b and the target in Fig. 2, there are four external inputs that are made for process noise $w(t)$ injection. The input in Bus 1 is used to emulate ambient operating conditions, by statistically varying the apparent power using a Gaussian noise with mean $\mu = 0$ and standard deviation $\sigma = 0.01$. This noise source is intended to mimic the random load changes

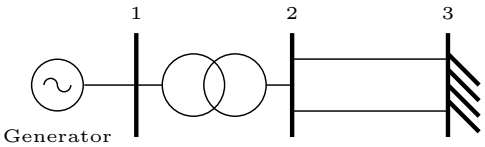

(a) Single-line diagram for the SMIB system.

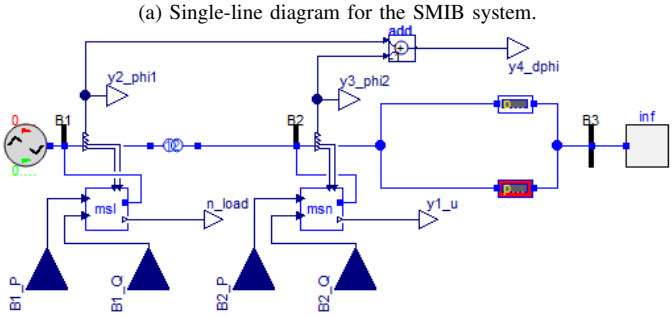

(b) Modelica implementation of the SMIB system exported as an FMU.

Fig. 1. Single Machine Infinite Bus (SMIB) system and its implementation in Modelica for FMI standard export.

that occur in a power system, acting as a constant low-level excitation to the electromechanical dynamics. It is chosen in this paper to be a white Gaussian in accordance to [3].

Meanwhile, for the probing signal, the pairs of inputs are connected to multi-sine injection blocks, which are then coupled to the buses. In Bus 2, the multi-sine signal is injected as reactive power and acts as the exciting signal $u(t)$, while the block connected to Bus 1 has a gain of zero, which means that it is inactive in these experiments. As mentioned before, in the first batch (first 60 seconds), the multi-sine signal is manually selected. The last 60 seconds (second batch) corresponds to the optimized input signal. Signal $u(t)$ aims to provide a model of what could be realized in the field by modulating the output of a Static Compensator (STATCOM). The output vector $y(t)$ is the angle difference between two nodes of the network (1 and 2). Measurement noise would be naturally added from the device measuring the Real-Time simulator outputs.

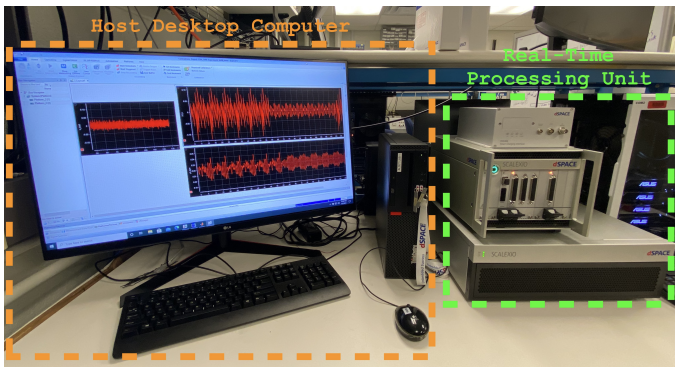

Fig. 2. Set-up for real-time simulation of Modelica models exported via the FMI standard.

The Modelica implementation is exported as a Co-Simulation (CS) FMU, which contains the source code for the model and a C-language variable-order ODE (CVODE) numerical solver, with tolerance 10^{-4}. The FMU is loaded into dSPACE's ConfigurationDesk (dCD) installed in the host computer where the model is configured. The noise $w(t)$ is

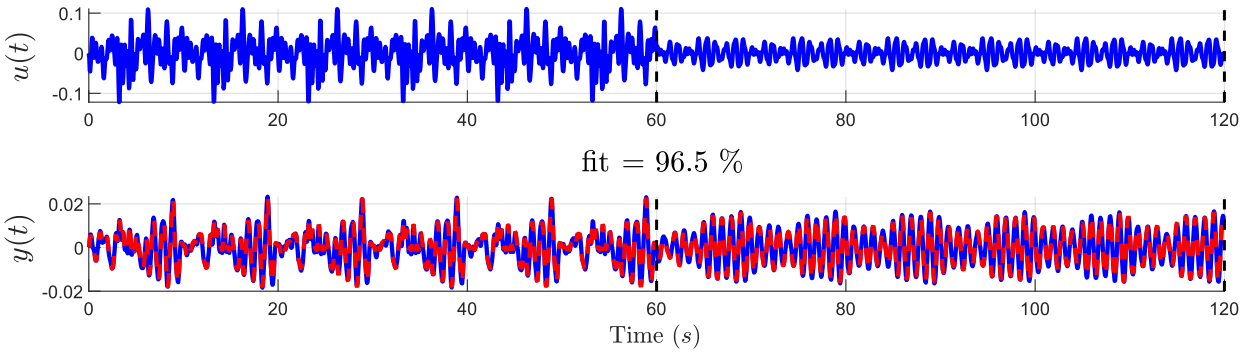

Fig. 3. Above: manually chosen excitation signal (first batch of 60 seconds) and optimized excitation signal (second batch from 60 seconds to 120 second). Below: measurements (blue) and output of the identified model (red) for Case One. Note that the depicted signals are relative to a nominal value.

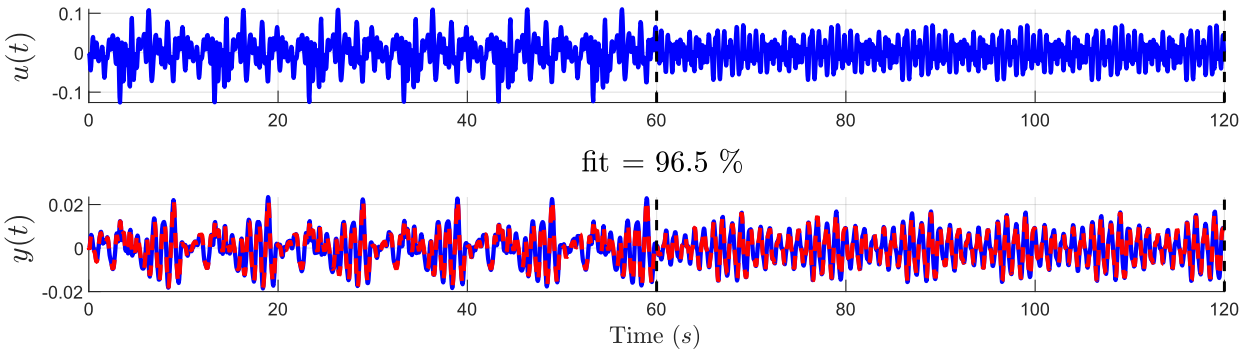

Fig. 4. Above: manually chosen excitation signal (first batch of 60 seconds) and optimized excitation signal (second batch from 60 seconds to 120 second). Below: measurements (blue) and output of the identified model (red) for Case Two. Note that the depicted signals are relative to a nominal value.

created in MATLAB. Both the FMU and the MATLAB model are within the dCD (i.e. in software), a time-step of 1 ms is selected and the model is built and loaded into a dSpace SCALEXIO LabBox. The physical set-up is depicted in Fig. 2, where the host desktop computer is highlighted in orange while SCALEXIO LabBox is highlighted in green.

The data obtained from the RT simulator is re-sampled and its trends and mean are removed before it is used for system identification. Moreover, the selected model structure for identification has 3 poles and 3 zeros.

IV. Case Study Results

A. Case One

With $c_2 = 0$, the optimization in Eq. (8) only minimizes the power in $u(t)$, while ensuring the upper bound η_i on the variance of the damping's estimation. The amplitudes of the multi-sine are depicted in Fig. 5 for the first (blue) and second batch (red). Clearly, the second batch contains less power content in $u(t)$, which is due to the optimization of Eq. (8). In fact, the power content of the excitation signal during the second batch is approximately 80% lower than during the first batch, where the excitation signal is manually chosen. The upper bound on the variance is selected in such way that the variances of the first and second batch are equivalent and set to an acceptable level.

The time domain results of the excitation signal $u(t)$ and measurement $y(t)$ are depicted in Fig. 3. The ordinate axis in $y(t)$ represents the percentage of deviation from nominal operation, which means that the experiment deviates less than

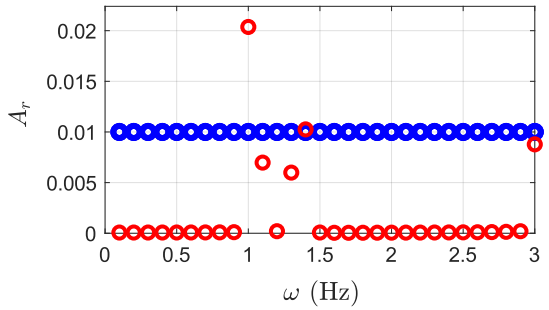

Fig. 5. Blue dots: manually chosen amplitudes of the multi-sine during the first batch. Red dots: optimized amplitudes of the multi-sine during the second batch for Case One.

2% from normal operating condition. The upper plot in Fig. 3 represents the manually chosen excitation signal from 0 to 60 s and the optimized input from 60 to 120 s. In the lower plot, the identified model's output, $\hat{y}(t)$, is presented in dashed red, while the measurements taken from the RT simulator are presented in blue. The fit calculated with11 is 96.5% in this case, while the cross validation between first and second batch has a fit of 89.6%. More importantly, the lowest damping value is estimated at 0.082 at frequency 1 Hz, while the true damping value is 0.079 at frequency 1.1 Hz, showing that the model is valid. In fact, note in Fig. 5 that the optimized $u(t)$ signal has most of its power content around 1 Hz, since exciting the network at that frequency yields more information. Furthermore, it is observed that the power content in $y(t)$ increases with approximately 20% during the second batch relative to the first batch. This is in fact undesired and can be

improved by introducing the weight c_2.

B. Case Two

Next, the second weight is selected to be $c_2 = 10^3$ and hence the power in both $u(t)$ and $y(t)$ is minimized, while the upper bound η_i on the variance of the damping estimation is ensured. The manually chosen amplitudes, in blue, and the optimized ones, in red, are shown in Fig. 6. Once again, the second batch contains less power in $u(t)$ compared to the power in the first batch, which is due to the optimization of the excitation signal.

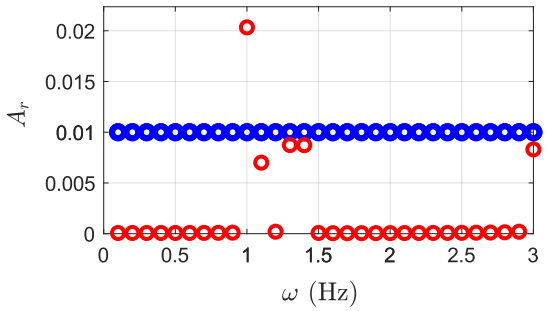

Fig. 6. Blue dots: manually chosen amplitudes of the multi-sine during the first batch. Red dots: optimized amplitudes of the multi-sine during the second batch for Case Two.

The time-domain results for this experiment are shown in Fig. 4. The ordinate axis represents a percentage of deviation form nominal operation, the upper plot represents $u(t)$, while the lower plot shows the real measurement value $y(t)$, in blue, and the identified output $\hat{y}(t)$, in dashed red. The identified output has a fit of 96.2%, while the cross validation between batches gives 90.7%. The damping value is estimated at 0.08 at frequency 1 Hz, while the true value is 0.079 at frequency 1.1 Hz. Here, the power content from the optimized $u(t)$ (second batch) is 40% lower than the manually chosen excitation signal (first batch), while the power content in the measured signal increases by $\approx 12\%$ compared to the first batch. Even though this is an increase, this is still a reduction of 40% compared to the first case (where $c_2 = 0$). In both cases, an equal upper bound on the variance of the damping is ensured, so no relaxation on the estimation's precision has to be introduced in order to change the power content in $u(t)$ or $y(t)$. Consequently, the power in the excitation signal in Case Two is increased during the second batch compared to Case One. This implies that, in order to obtain a certain accuracy for the damping estimation, it is possible to reduce the power in the measurement (deviation from nominal operation) by tuning the ratio c_1/c_2. Although it is then possible that the power content in the excitation signal increases. This implies that, via the optimization defined in Eq. (8), a clear trade-off can be made in the power content of the measurement and excitation signal, while ensuring accurate damping estimations.

V. Conclusions

This paper presents a framework for designing real-time hardware-in-the-loop experiments using Modelica and the FMI standard. Such a framework allows for relatively easy testing of system identification techniques before real field testing is performed. The Modelica model of the network is built using the OpenIPSL and the exported FMU is loaded into SCALEXIO LabBox for RT simulation. The system identification technique with optimized input signals was implemented and performed successfully. The first conducted experiment showed that it is possible to optimize $u(t)$ in terms of minimizing the power of the probing signal, just by adjusting the weight c_1. The second case had a power increase in $u(t)$ compared to the first. However, the power in $y(t)$ is reduced substantially, thereby minimizing the impact on the power network. This is thanks to the introduction of the weight c_2. The experiment demonstrates that the weights c_1 and c_2 allow the user to choose for more/less power in $u(t)$ or $y(t)$, while ensuring precise damping estimations.

References

[1] J. F Hauer and R. L. Cresap, "Measurement and modeling of pacific AC intertie response to random load switching", *IEEE Transactions on power apparatus and systems*, vol. 1, no. 1, Jan., pp. 353-359, 1981.

[2] L. Dosiek and J. W. Pierre, "Estimating electromechanical modes and mode shapes using the multichannel ARMAX model", *IEEE transactions on Power Systems*, vol. 28, no. 2, Apr., pp. 1950-1959, 2013.

[3] N. Zhou, J. W. Pierre, J. F. Hauer, "Initial results in power system identification from injected probing signals using a subspace method", *IEEE Transactions on Power Systems*, Vol. 21, No. 3, Jul., pp. 1296-1302, 2006.

[4] B. J. Pierre *et al.* "Open-loop testing results for the pacific DC intertie wide area damping controller", In Proc. 2017 IEEE Manchester PowerTech, 2017, pp. 1-6.

[5] S. A. N. Sarmadi and V. Venkatasubramanian, "Inter-area resonance in power systems from forced oscillations", *IEEE Transactions on Power Systems*, vol. 31, no. 1, Feb., pp. 378-386, 2015.

[6] J. F Hauer and F. Vakili, "An oscillation detector used in the BPA power system disturbance monitor", *IEEE Transactions on Power Systems*, vol. 5, no. 1, Feb., pp. 74-79, 1990.

[7] M. Donnelly *et al.* "RMS-energy filter design for real-time oscillation detection", In Proc. 2015 IEEE PES GM, 2015, pp. 1-5.

[8] J. W. Pierre *et al.* "Probing signal design for power system identification", *IEEE Transactions on Power Systems*, vol.25, no. 2, Nov., pp. 835-843, 2009.

[9] V. Perić, X. Bombois and L. Vanfretti, "Optimal multisine probing signal design for power system electromechanical mode estimation", In Proc. 50th Hawaii International Conf. on System Sciences, 2017, pp. 1-9.

[10] S. Boersma, X. Bombois, L. Vanfretti, J. C. Gonzalez-Torres, A. Benchaib, "Probing signal design for enhanced damping estimation in power networks", *International Journal of Electrical Power & Energy Systems*, vol. 129, Jul., pp 1-15, 2021.

[11] E. Rebello, L. Vanfretti and M. S. Almas, "Experimental Testing of a Real-Time Implementation of a PMU-Based Wide-Area Damping Control System," in IEEE Access, vol. 8, pp. 25800-25810, 2020.

[12] Modelica Association, "Modelica Language", Available: `https://modelica.org/modelicalanguage.html`, [Accessed: July 8 2021].

[13] Modelica Association Project, "Functional Mock-up Interface", Available: `https://fmi-standard.org/`, [Accessed: July 8 2021].

[14] K. J. Åström and T. Bohlin, "Numerical identification of linear dynamic systems from normal operating records", *IFAC Proceedings Volumes*, vol. 2, no. 2, Sep., pp. 96-111, 1965.

[15] T. Söderström and P. Stoica, *System Identification*, Prentice-Hall International, 1989.

[16] L. Ljung, "Asymptotic variance expressions for identified black-box transfer function models", *IEEE Transactions on Automatic Control*, vol. 30, no. 9, Sep., pp. 834-844, 1985.

[17] M. Baudette, M. Castro, T. Rabuzin, J. Lavenius, T. Bogodorova and L. Vanfretti, "OpenIPSL: Open-instance power system library—update 1.5 to iTesla power systems library (iPSL): A modelica library for phasor time-domain simulations", *SoftwareX*, vol. 7, Jan., pp. 34-36, 2018.